

# Numerical Simulation of Vortex Ring Interactions with Solid Wall

Debojyoti Ghosh\* and James D. Baeder†

*University of Maryland, College Park, MD 20742, USA*

An attempt is made to study flows dominated by multiple vortical structures and their interactions with a solid wall. The leapfrogging of co-rotating vortex rings and the interactions of a vortex ring with free-slip and no-slip walls have been studied in literature. In the present study, the interactions of multiple vortex rings with a solid wall are simulated numerically to understand the effect of mutual interactions between vortex rings on their interactions with the boundary layer. A three-dimensional Cartesian incompressible Navier-Stokes solver based on the fractional-step algorithm is used. An upwind reconstruction along with the Weighted Essentially Non-Oscillatory interpolation is used for the convective flux terms to yield non-oscillatory results at high Reynolds numbers. High order Runge Kutta time stepping is used for time-accurate simulations. The governing equations are solved on a staggered mesh to avoid pressure-velocity decoupling issues. The algorithm is validated for the impingement of a vortex ring on a solid wall with experimental and computational results in literature. Results are then presented for the interactions of two and multiple co-rotating, coaxial rings with a solid wall.

## I. Introduction

The flow around a rotorcraft is highly unsteady, consisting of vortices shed from the blade tips. The behavior of these vortex rings in terms of their mutual interactions and interactions with a solid ground determines the flow in the wake of a rotor in ground effect. Accurate simulation of vortex-dominated flows is necessary to understand this flowfield. While the rotor wake consists of helical vortex rings convecting to the ground, studying the interactions of axis-symmetric vortex rings provide insightful results. The motivation of the present study is to study the interactions of multiple vortical structures with a solid wall.

The formation, convection and interactions of vortex rings with each other as well as solid walls have been studied in literature.<sup>1-3</sup> The mutual interactions of co-rotating vortex rings and the interactions of a vortex ring with a solid wall under inviscid and viscous conditions are relevant to the present study. The behavior of two co-rotating vortex rings has been extensively studied.<sup>4-6</sup> The trailing vortex ring causes the leading ring to expand and consequently slow down while the leading ring causes the trailing ring to contract and accelerate. Under inviscid conditions, this causes the trailing ring to slip through the leading ring and this motion repeats itself indefinitely, causing a leapfrogging behavior.<sup>4</sup> However, for viscous flows, the behavior depends on the Reynolds number, the initial separation and the core thickness of the rings.<sup>5,6</sup> Early experiments at low Reynolds numbers reported the merging of the two rings as the trailing ring caught up with the leading ring. Under specific conditions, however, a finite number of leapfrogging cycles are observed before core distortion and viscous dissipation causes the rings to merge into a single ring.

The ideal fluid theory models the inviscid approach of a vortex ring towards a solid wall using the image plane technique.<sup>7</sup> The problem is equivalent to two vortex rings of opposite circulation approaching each other along a common axis. It is predicted that the rate of approach decreases as the ring nears the wall and the diameter increases leading to a decrease in the core size. However, for a viscous fluid, the evolution is quite different due to the interaction of the vortex ring with the wall boundary layer. Several experimental investigations have been reported focusing on the normal impingement of a ring on a solid wall.<sup>7-10</sup> In all these studies, it is observed that the vortex ring induces a surface vorticity with an opposite sense of

---

\*Graduate Student, Applied Mathematics & Statistics, and Scientific Computation, ghosh@umd.edu

†Associate Professor, Department of Aerospace Engineering and Associate Fellow, AIAA, baeder@umd.edu.

circulation in the boundary layer. As the ring approaches the wall, the surface vorticity layer intensifies and eventually ejects a secondary vortex ring. Depending on the Reynolds number, the ejection of a tertiary ring is also possible. The induced velocity field of the secondary and tertiary rings affect the trajectory of the primary ring near the wall. The secondary and tertiary rings roll up around the primary ring and eventually coalesce. Similar results have been observed in computational studies.<sup>11,12</sup>

In the present study, a Cartesian incompressible Navier-Stokes solver<sup>13</sup> based on the fractional step algorithm is used to study the interactions and convection of vortices as well as their impingement on solid walls. The governing equations are the incompressible Navier Stokes equations in their primitive form.<sup>14</sup> While several different formulations exist for the Navier Stokes equations, the primitive variable formulation is chosen due to its relative ease of implementation. Several numerical techniques have been proposed in literature which can be classified as the pressure correction schemes,<sup>15,16</sup> the artificial compressibility techniques<sup>16,17</sup> or the projection methods.<sup>18,19</sup> The projection method, also known as the fractional step algorithm<sup>20</sup> is used in the present study because of its applicability to unsteady problems.

The numerical algorithm has been previously validated for benchmark incompressible flow problems.<sup>13</sup> In the present study, the algorithm is validated on vortex dominated flows for which results are available in literature. The algorithm is used to simulate the inviscid interaction of two co-rotating vortex rings and the inviscid impingement of a vortex ring on a solid wall. The results are shown to be consistent with theoretical predictions. The algorithm is also validated for viscous interactions of vortical structures with a solid wall. A two-dimensional interaction of a vortex dipole with a wall is studied as it encapsulates many of the flow features of a vortex ring interacting with a wall (except the ring expansion and consequent core shrinking). The interaction of a vortex ring with a solid wall is studied at two different Reynolds numbers and the results are compared with those in literature. Based on these results, the interactions of two and multiple rings with a solid wall are simulated, which are believed to be a combination of the above behaviors. Results are shown for different Reynolds numbers and initial separations and an attempt is made to understand the effect of these parameters on the flow.

## II. Governing Equations

The Navier Stokes equations<sup>14</sup> govern the physics of incompressible flow. They comprise of the conservation equations for mass, momentum and energy. The conservation of mass, for a constant density, can be expressed as

$$\nabla \cdot \mathbf{u} = 0 \quad (1)$$

and the equations for the conservation of momentum are given by

$$\frac{\partial \mathbf{u}}{\partial t} + (\mathbf{u} \cdot \nabla) \mathbf{u} = -\nabla \left( \frac{p}{\rho} \right) + \nu \nabla^2 \mathbf{u} \quad (2)$$

$\mathbf{u}$  is the velocity vector,  $p$  is the pressure,  $\rho$  is the density and  $\nu$  is the coefficient of kinematic viscosity. The equation for energy conservation is decoupled from the momentum equations and is not solved as a part of the solution process.

## III. Numerical Algorithm

A high order accurate algorithm based on upwind flux reconstruction was developed focusing on high Reynolds number and inviscid incompressible flows.<sup>13</sup> The algorithm is based on the fractional step procedure where the momentum equations are solved in two stages.<sup>20</sup> The predictor step involves the solution of the convective and viscous terms and an intermediate velocity field is computed which is the solution of

$$\frac{\partial \mathbf{u}}{\partial t} = -(\mathbf{u} \cdot \nabla) \mathbf{u} + \nu \nabla^2 \mathbf{u} \quad (3)$$

The intermediate velocity field  $\mathbf{u}^*$  thus obtained has a non-zero divergence. The corrector step is used to calculate the zero divergence projection of this velocity field,

$$\frac{\partial \mathbf{u}}{\partial t} = -\nabla \phi \quad (4)$$

In the corrector step,  $\phi$  is the solution of the Poisson equation

$$\nabla^2 \phi = \frac{1}{\Delta t} \nabla \cdot \mathbf{u}^* \quad (5)$$

and is called the “pseudo-pressure”.  $\Delta t$  is the time step size for the numerical algorithm. It should be noted that  $\phi$  is a mathematical quantity introduced to enforce the divergence-free condition on the velocity field, given by Eq. (1) and is not the physical pressure.<sup>20</sup>

The above equations are discretized on a staggered Cartesian mesh to prevent the pressure-velocity decoupling issues seen on collocated meshes. The convective terms in the predictor step given by Eq. (3) are integrated in time using the second order Adams-Basforth (AB) or the third order Low Storage Runge Kutta (RK) schemes. At low Reynolds numbers, second order central differences are used for spatial discretization. At higher Reynolds numbers and for inviscid flow cases, central differencing yields oscillatory solutions and the physical viscosity is insufficient to dampen out the errors. Therefore, an upwind reconstruction is used based on the velocity component normal to the interface.<sup>13</sup> High order interpolation is used to calculate the interface fluxes. The Weighted Essentially Non-Oscillatory (WENO)<sup>21</sup> scheme is used to prevent oscillations for problems with large gradients.

The viscous terms are discretized in space using second order central differences. At low Reynolds numbers, to avoid time step restrictions due to the diffusion number, the Crank-Nicholson time integration is used for the viscous terms. The resulting system of equations is solved iteratively using the Strongly Implicit Procedure (SIP).<sup>22</sup> At high Reynolds numbers, it is sufficient to treat the viscous terms explicitly. However, the iterative procedure for the implicit scheme is seen to converge rapidly and is thus retained. Similarly, for the corrector step given by Eq. (4), second order central differencing is used for the gradient term.

The solution of the Poisson equation for the pseudo-pressure, given by Eq. (5), is the most expensive computationally. The Laplacian and divergence operators are discretized using second order central differences. Along with homogeneous Neumann boundary conditions, the resulting system is ill-conditioned. The SIP algorithm is used, however, unlike in the predictor step, convergence is slow.

## IV. Validation

The algorithm has been validated over benchmark incompressible flow problems in earlier studies.<sup>13</sup> Results were obtained and compared for the lid driven square cavity and the inviscid shear layer problems. The accuracy and convergence was tested on the isolated Taylor vortex convection case for which the exact solution is available. The algorithm was seen to perform satisfactorily for both viscous and inviscid flows. In the present section, the algorithm is validated for vortex-dominated flows. The inviscid leapfrogging motion of two co-rotating vortex rings is simulated. The velocity field of the leading ring causes the trailing ring to contract and slip through, while it expands due to the velocity field of the trailing ring. This pattern is repeated indefinitely for inviscid flows whereas core distortion due to viscosity causes the rings to eventually merge after a finite number of passes depending on the Reynolds number and initial separation. The interaction of a vortex ring with a free-slip (inviscid) wall boundary is studied and the results are consistent with the ideal fluid theory predictions. The algorithm is validated for viscous interactions of vortices with a solid wall. The two-dimensional vortex dipole rebound from a solid wall is studied and results compared to those in literature. This is a simplified representation of the three-dimensional ring impingement lacking the core straining that occurs for an expanding or contracting vortex ring. The three-dimensional case of a single ring impacting a solid wall is simulated at two different Reynolds numbers. The present results are compared with previous experimental and computational studies.

### IV.A. Leapfrogging Motion of Co-Rotating Vortex Rings

In this problem, the inviscid interactions between two coaxial vortex rings with the same sense of circulation is studied. A leapfrogging motion of two rings around each other is predicted for large, thin rings in the inviscid limit.<sup>4</sup> The trailing ring contracts and slips through the leading ring. This motion is repeats indefinitely for inviscid flows. In the presence of viscosity, the strength of the vortex rings gradually decrease and they eventually coalesce to form a single ring due to the mutual interactions. The ratio of the core radius to the ring diameter, initial separation and the Reynolds number determine the number of leapfrogging cycles

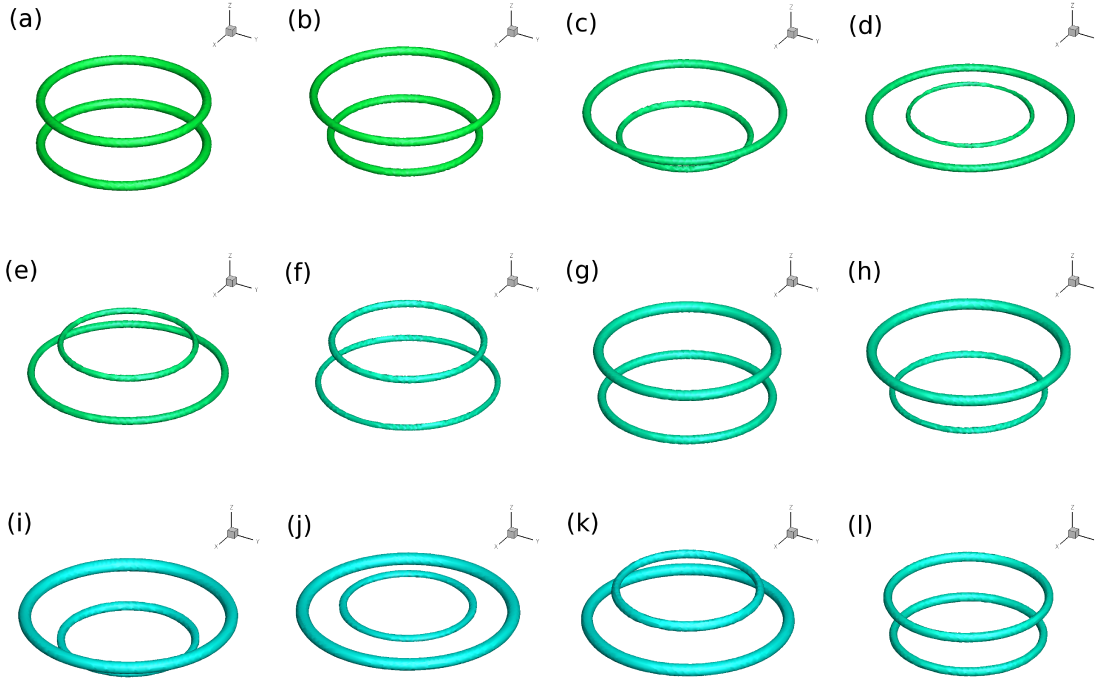


**Figure 1. Leapfrogging of Coaxial Vortex Rings**

before the rings coalesce.<sup>5</sup> Thicker rings tend to coalesce sooner whereas large, thin rings leapfrog around each other for longer times.

In the present case, the initial flow consists of two identical rings, each with a Gaussian azimuthal vorticity distribution along the core cross-section given by

$$\omega(x, y, z) = \frac{1}{\pi a^2} \exp[-(\frac{r}{a})^2] \quad (6)$$

where  $\omega$  is the vorticity magnitude along the normal to the cross-section,  $r$  is the distance from the center of the core and  $a$  is the core radius. A ring thickness  $a/R$  of 0.05 is used where  $R$  is the ring radius. A cubic domain of side  $5R$  is chosen with periodic boundary conditions on all boundaries and the initial separation between the rings is taken as  $0.6R$ . A  $144 \times 144 \times 144$  grid is used to discretize the domain and results are obtained using the 5th order WENO scheme and 3rd order RK time stepping. Figure 1 show the leapfrogging behavior for one complete cycle. The iso-surfaces of the vorticity magnitude are plotted and the color shows the gradual decrease in the vortex strength due to numerical dissipation. The algorithm is seen to accurately capture the leapfrogging behavior and its performance for flows with concentrated vorticity is demonstrated.

#### IV.B. Inviscid Wall Interactions

The inviscid interaction of a vortex ring with a solid wall is studied. The problem can also be modeled as two counter-rotating vortex rings approaching each other by considering the free-slip wall as a plane of reflection. The velocity field of the reflected vortex ring causes the primary vortex ring to expand as it approaches the wall, thus causing its core to shrink. The self-induced velocity of the vortex ring reduces as it expands causing it to asymptotically approach the wall.

Figure 2 shows the vorticity magnitude iso-surfaces and cross-sectional contours as a vortex ring approaches a free-slip wall. The flow is initialized as a vortex ring with cross-sectional vorticity distribution given by Eq. (6). A ring thickness  $a/R$  of 0.413 is used and the core thickness is taken to yield a maximum vorticity magnitude of 35 non-dimensional units. The initial height above the ground is  $2.4R$ . The computations are carried out on a  $144 \times 144 \times 200$  clustered grid with six grid points across the vortex core initially.

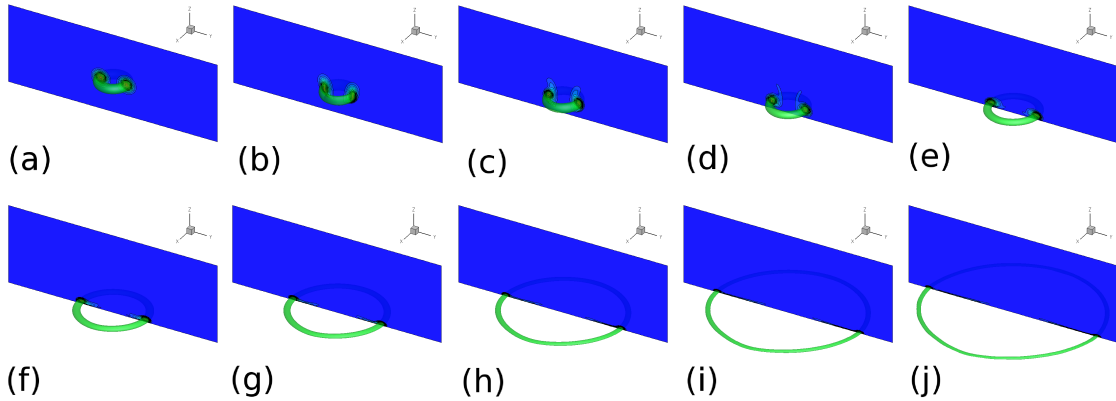


**Figure 2. Inviscid Interaction of a Vortex Ring with a Wall**

As the solution progresses, the core shrinks and in the final solution, it is resolved by three grid points. Inviscid wall (reflection) boundary conditions are imposed on the bottom boundary and extrapolation boundary conditions are used at all other boundaries. The problem is solved using the 5th order WENO scheme and 3rd order RK time stepping. The expansion of the ring and the corresponding shrinking of the core can be observed as the ring approaches the solid wall.

#### IV.C. Viscous Wall Interactions

##### IV.C.1. Vortex Dipole

The interaction of a vortex dipole with a wall<sup>23</sup> illustrates many of the mechanisms seen in the interaction of a vortex ring with a wall. As the vortex dipole approaches the solid surface, it induces a surface vorticity of the opposite sign in the boundary layer. The problem is characterized by the ejection of secondary and tertiary vortices which then interact with the primary vortices. In the present study, the flow is initialized as a vortex dipole in stagnant flow with a Gaussian vorticity distribution given as

$$\omega(x, y) = \pm \frac{1}{\pi a^2} \exp\left[-\frac{(x - x_c)^2 + (y \pm y_c)^2}{a^2}\right] \quad (7)$$

where  $\omega$  is the vorticity magnitude and  $x$  is the axis normal to the wall. The vortices are centered at  $(x_c, \pm y_c)$  with a core radius of  $a$ . The problem is solved at a circulation based Reynolds number ( $Re = 1/\nu$ ) of 1800. The domain is specified as  $-\delta \leq x \leq \delta$  and  $0 \leq y \leq 2\pi\delta$  and the initial separation of the vortices is  $\delta/3$ .<sup>24</sup> The core radius of the vortices is  $a = \delta/9$ . The problem is solved on a  $128 \times 256$  mesh. Periodic boundary conditions are applied at  $y = 0, 2\pi\delta$ , solid wall boundary conditions are applied at  $x = -\delta$  and extrapolation is used at  $x = \delta$ .

Figure 3 shows the evolution of the problem using 2nd order spatial discretization and 3rd order RK time stepping. The out-of-plane vorticity contours are plotted. It can be seen that the primary vortices induce a boundary layer vorticity region as they approach the wall. The boundary layer vorticity, having an opposite sense of circulation, causes the primary vortices to move apart. They are ejected from the boundary layer as secondary vortices and interact with the primary vortices. At a later stage, tertiary vortices are also seen to be ejected. However, the vortices diffuse with time due to the viscosity in the flow. The results agree with those in literature.<sup>23, 24</sup>

##### IV.C.2. Vortex Ring

The impingement of a single vortex ring on solid wall is studied in this case. As the ring approaches the wall, it expands in size and induces a boundary layer at the wall. Depending on the Reynolds number, the vorticity in the boundary layer can grow till it gets ejected in form of a secondary ring, which rolls around the primary ring. A tertiary ring ejection may also be observed for higher Reynolds number flows. In the present study, this interaction of the ring with a solid wall is studied at two different Reynolds numbers. The initial conditions consist of an isolated vortex ring with a cross-sectional vorticity distribution given by

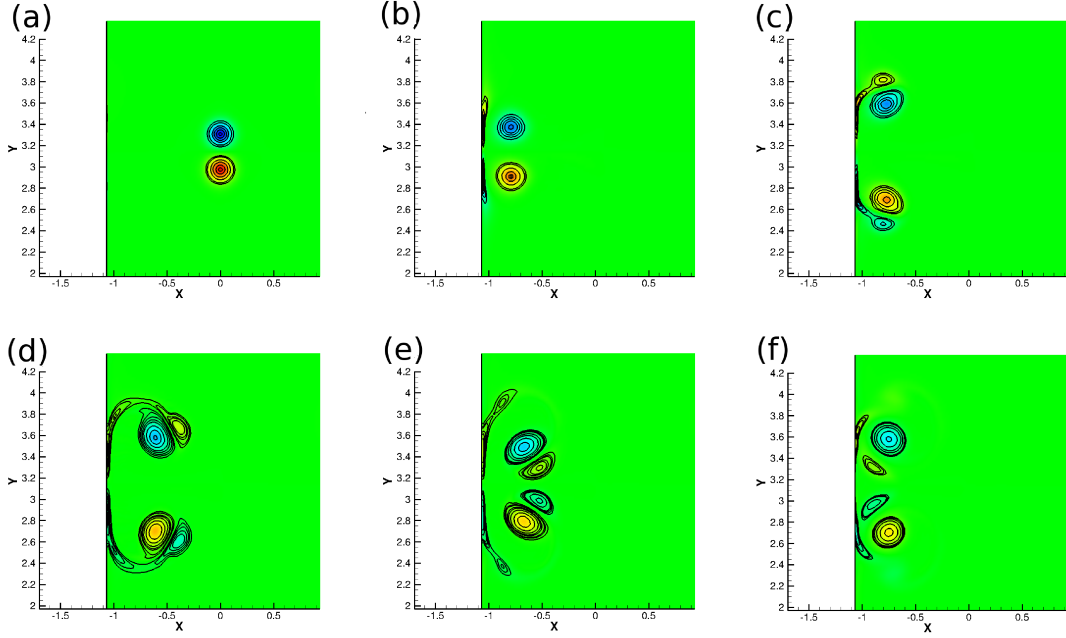


**Figure 3. Rebound of Vortex Dipole from Wall at Reynolds number of 1800**

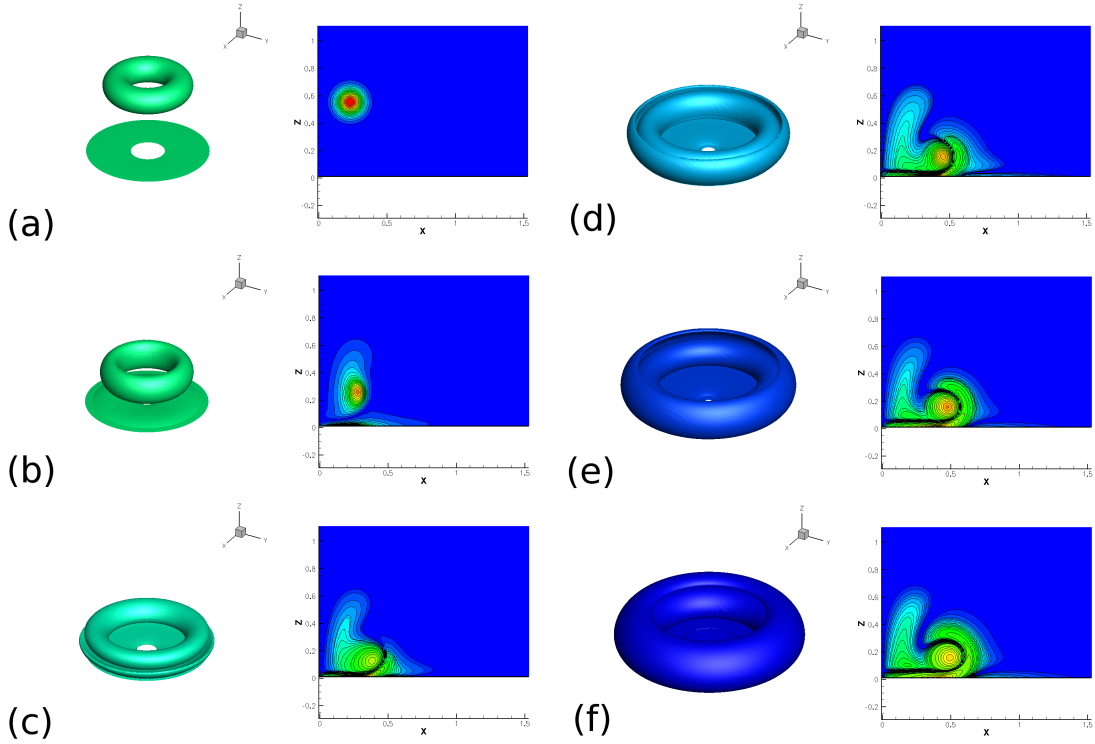


**Figure 4. Vortex Ring Impingement on Wall at Reynolds number of 564**

Eq. (6). The core radius is taken to yield a maximum vorticity magnitude of 35 for unit circulation.<sup>11</sup> The ring radius  $R$  is taken as  $a/0.413$  and the initial height of the ring above the ground is taken as  $2.4R$ . The problem is simulated on a clustered mesh of dimensions  $144 \times 144 \times 200$ . Solid wall boundary conditions are imposed on the bottom ( $z = 0$ ) boundary and extrapolation is used at all other boundaries.

The problem is simulated for two different circulation-based Reynolds numbers. Figure 4 shows the

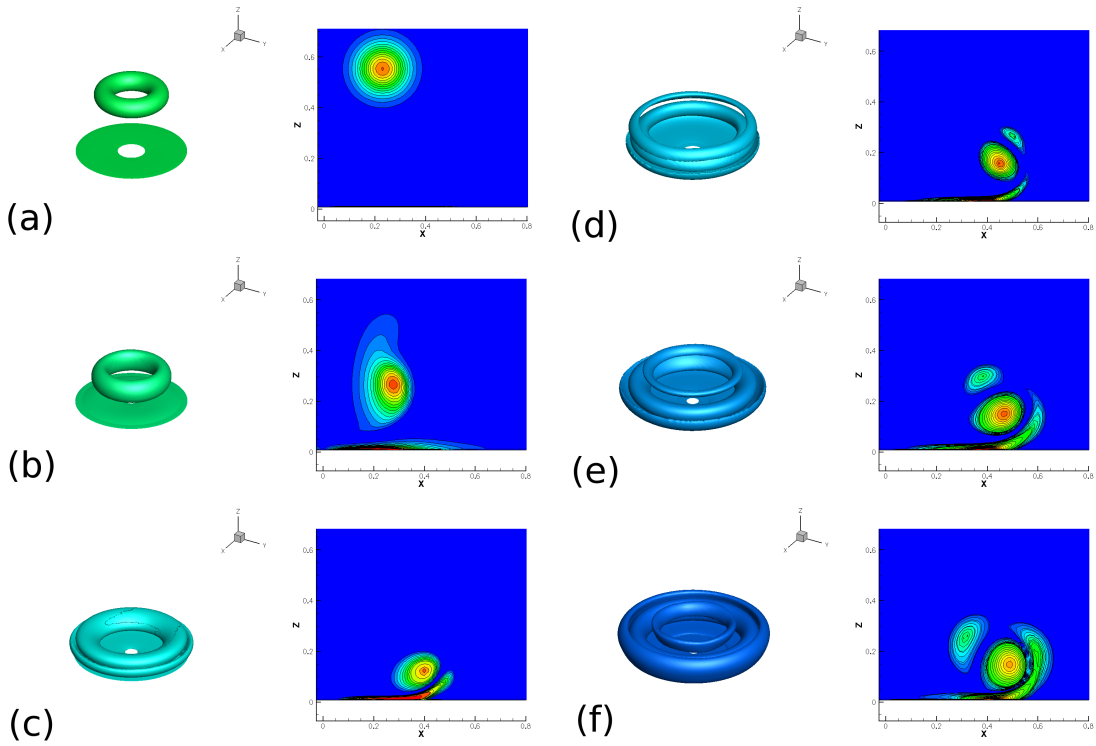


**Figure 5.** Vortex Ring Impingement on Wall at Reynolds number of 1250

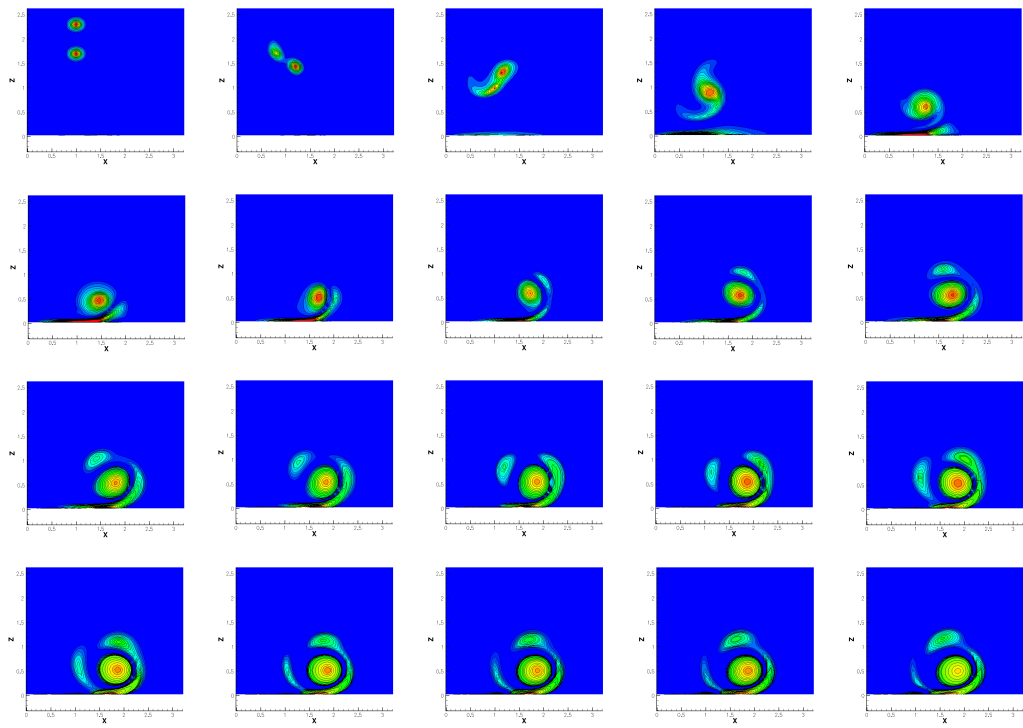
evolution of the problem at a Reynolds number of 564. The results are computed using 2nd order spatial differencing and 3rd order RK time stepping. At this low Reynolds number, the ring induces a boundary layer vorticity which wraps around the primary ring. The left-hand side of each image shows the vorticity magnitude iso-surfaces and the right hand side shows a contour plot of the vorticity magnitude on an azimuthal slice. The color of the iso-surfaces show a gradual dissipation of the vortices as expected. The induced vorticity in the boundary layer is not strong enough to get ejected and form a separate secondary ring.

Figure 5 shows the evolution for a higher Reynolds number of 1250. The results are obtained using the 5th order upwind WENO scheme with 3rd order RK time stepping. At a higher Reynolds number, the induced vorticity in the boundary layer is much stronger and the ejection and formation of a secondary ring can be clearly seen. The secondary ring circles around the primary one while a tertiary ring can be seen to be forming.

The results obtained are compared with those in literature<sup>11</sup> and good agreement is seen. The characteristic features of the ring-wall interactions are seen to be accurately captured.

## V. Results

The previous section demonstrated the performance of the algorithm on vortex dominated flows which are pertinent to the simulation of multiple vortex rings interacting with a solid wall. The inviscid leapfrogging of two co-rotating vortex rings was simulated as an example of the mutual interaction of two vortex rings. The inviscid and viscous interactions of a vortex ring with a solid wall were studied and results validated with results in literature. Based on these results, the simulation of multiple rings interacting with a solid wall is attempted. Initially, the interaction of two co-rotating, coaxial rings with a solid wall is studied. The problem is simulated at two different Reynolds numbers and initial separation distances. These parameters affect the mutual interaction of the two rings in terms of leapfrogging or coalescing and thus affect the interactions with the wall. Subsequently, the simulation of multiple vortex rings interacting with a solid wall is attempted. The simulation is carried out for two different initial separations and representative results are shown.



**Figure 6.** Two Rings Impingement on Wall at Reynolds number of 564 for Initial Separation of  $0.6R$  (Time evolution is from left to right and top to bottom)

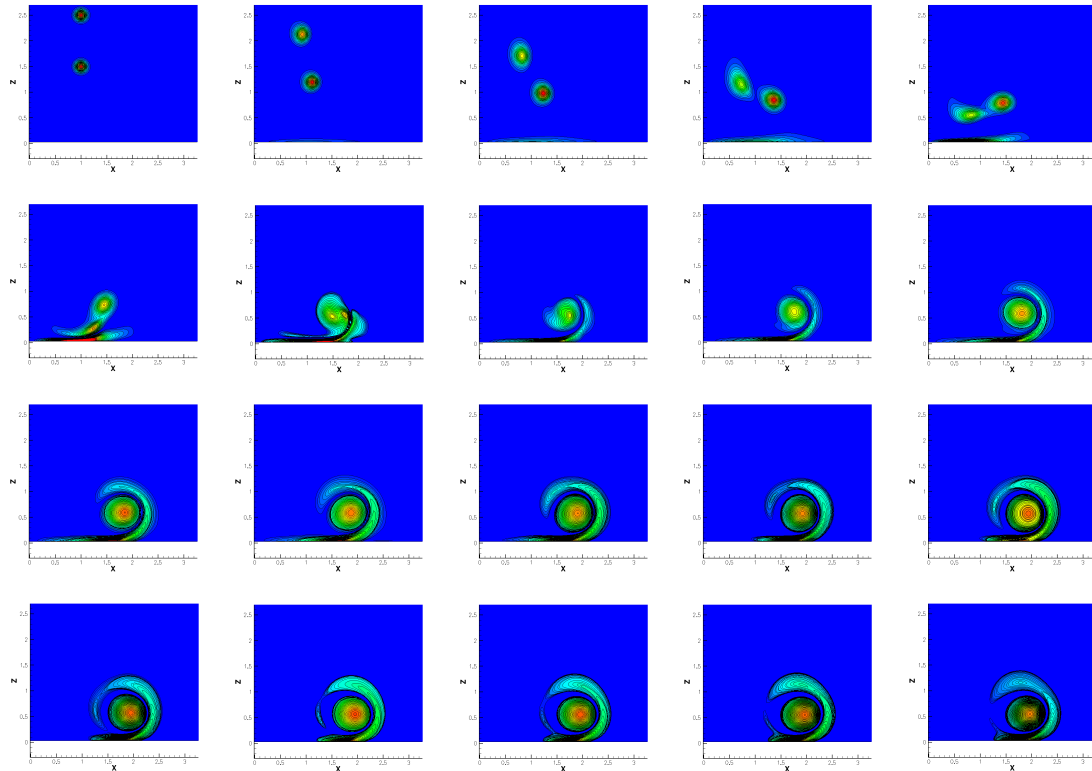


**Figure 7.** Two Rings Impingement on Wall at Reynolds number of 564 for Initial Separation of  $1.0R$  (Time evolution is from left to right and top to bottom)

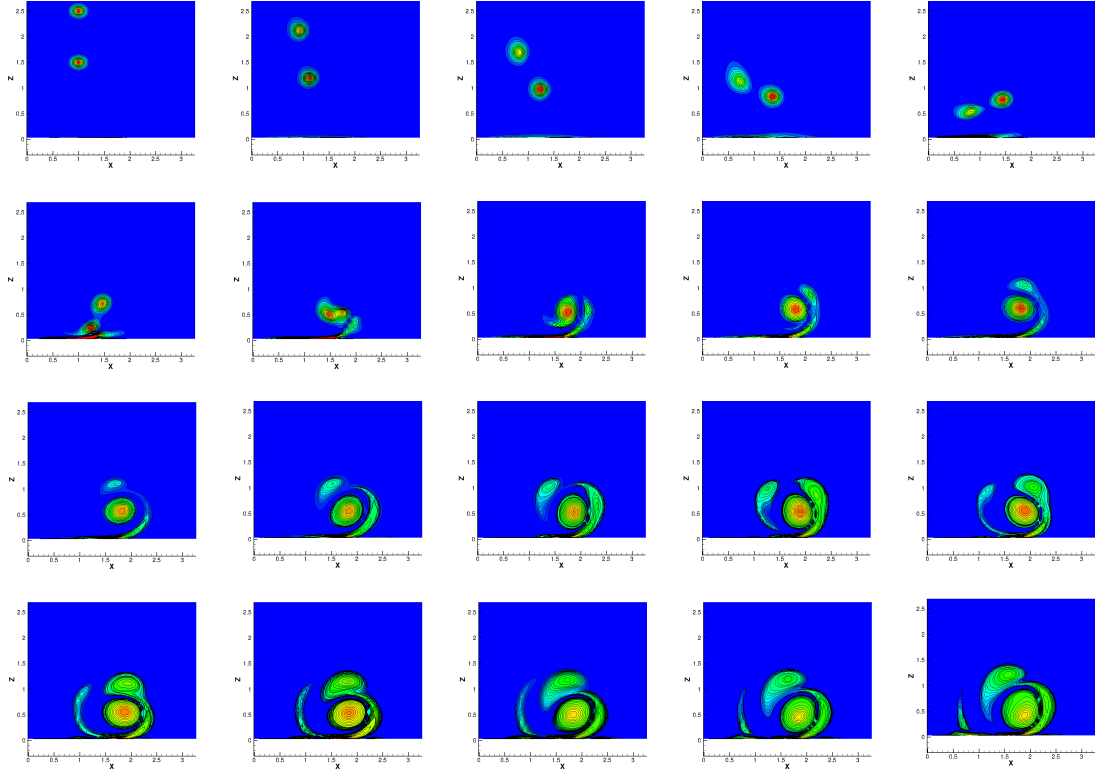


**Figure 8.** Two Rings Impingement on Wall at Reynolds number of 1250 for Initial Separation of  $1.0R$  (Time evolution is from left to right and top to bottom)

### V.A. Interactions of Two Rings with a Wall

The impingement of a pair of co-rotating vortex rings on a solid wall is studied. The approach of an isolated vortex ring towards a solid wall is characterized by the formation of a ground boundary layer and a creation of surface vorticity with an opposite sense of circulation. In the present case of two vortex rings, the initial separation and the Reynolds number affect the mutual interaction of the two rings and consequently their impingement on the wall. It is expected that for small initial separations and at low Reynolds numbers, the two rings will coalesce to form a single ring prior to their impingement on the wall and thus, the flow will be similar to a single vortex ring impingement. However, at higher Reynolds number and/or for higher initial separation, the rings will leapfrog as they impinge on the wall. The velocity field of one of the rings is expected to push the other ring towards the boundary layer, causing a stronger interaction while the velocity field of the latter will push the former away from the wall. In the present study, the problem is studied at two different Reynolds numbers and two initial separations.

The flow is initialized for all cases as two rings, each with a cross-sectional vorticity distribution given by Eq. (6). The ring thickness  $a/R$  is 0.1 and the initial mean height is  $2R$ . Figure 6 shows the evolution of two vortex rings initially separated by a distance of  $0.6R$  at a circulation-based Reynolds number of 564. The vorticity magnitude contours are plotted for an azimuthal plane. The domain is discretized using a  $144 \times 144 \times 200$  clustered grid and computations are carried out using the 5th order WENO scheme and the 3rd order RK time stepping. No-slip boundary conditions are applied at the bottom boundary and extrapolation boundary conditions are applied at all other boundaries. It is observed in this case that the two rings merge into a single ring before the impingement and the flow behavior after the impingement is similar to that of an isolated ring. However, the two primary rings coalesce to form a single ring that induces a stronger counter-rotating secondary vortex in the boundary layer, compared to the case of an isolated ring at the same Reynolds number. The impingement of a single ring at this Reynolds number causes the boundary layer to wrap around the primary ring but the interaction is not strong enough to eject a secondary ring. The impingement of two rings causes the ejection of a secondary ring and a tertiary ring. The velocity field of the coalesced primary ring causes the secondary ring to revolve around it and rejoin the boundary

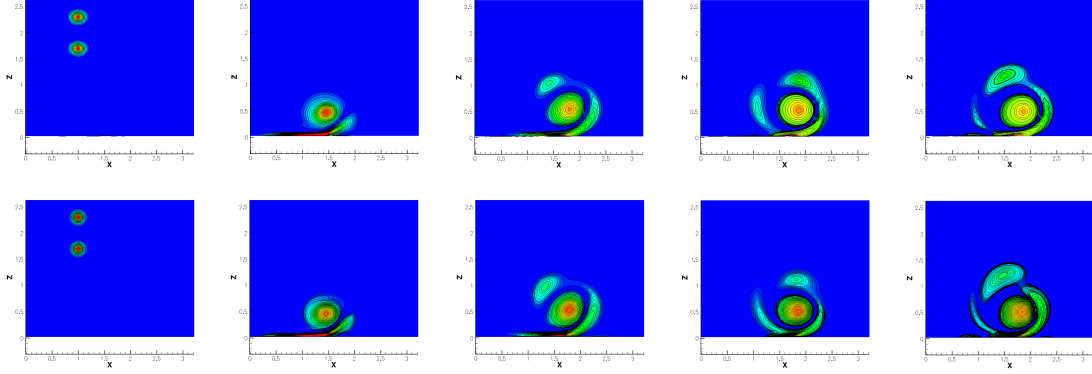


**Figure 9.** Comparison of solutions obtained for two different mesh sizes -  $144 \times 144 \times 200$  (top row) and  $300 \times 300 \times 200$  (bottom row) (Time evolution is from left to right)

layer.

Figure 7 shows the evolution of the rings for an initial separation of  $1.0R$ . The computations are carried out on a  $300 \times 300 \times 200$  grid. The larger initial separation allows for a more pronounced leapfrogging and the vortex rings do not coalesce before their impingement on the wall. It is observed that the velocity field of the initially leading ring pushes the initially trailing ring deeper into the boundary layer, while the velocity field of the latter pushes the former away from the wall. The two rings are observed to coalesce after the impingement of the initially trailing ring on the boundary layer. Overall, a weaker interaction is observed between the rings and the boundary layer and no secondary or tertiary rings are ejected. This can be explained by noting that the vorticity in the boundary layer has an opposite sense of circulation and the collision of one of the primary ring with the surface vorticity results in the weakening of both. The problem is studied for the same initial separation and at a higher Reynolds number of 1250, as shown in Fig. 8. Initially, a similar behavior is seen where the initially trailing ring is pushed deeper into the boundary layer while the initially leading ring is pushed away. The two primary rings merge after the impingement. At a higher Reynolds number, the interactions are stronger resulting in the ejection of secondary and tertiary vortex rings. It is observed that at later times, the secondary ring induced a surface vorticity of its own which affects its trajectory. This is not as pronounced in the previous cases studied.

A grid convergence test is carried out to test the effect of grid refinement on the solution. Figure 9 shows the solution for the evolution of two rings at a Reynolds number of 564 with an initial separation of  $0.6R$ . The top row shows the solution (corresponding to every fifth plot in Fig. 6, starting from the first) obtained on a  $144 \times 144 \times 200$  grid and the bottom row shows the same solutions obtained on a  $300 \times 300 \times 200$  grid. While the results are qualitatively similar, the fine grid solution predicts a faster motion for the secondary vortex ring. This is expected as the numerical diffusion in the coarse grid solution leads to an under-prediction of the velocity field of the primary ring.

### V.B. Interactions of Multiple Rings with a Wall

The impingement of multiple vortex rings on a solid wall is studied. The flow consists of an infinite train of vortex rings approaching the wall. While the separation between rings and the Reynolds number are expected to affect the mutual interaction between rings, the trajectories of the secondary and tertiary vortices ejected from the boundary layer are expected to be affected by the incoming vortex rings. In the present study, an infinite train of incoming vortex rings is realized by initializing the flow to a single ring at a given initial height above the wall and adding vortex rings to the solution at periodic intervals. The ring thickness  $a$  is  $0.1R$  and an initial height of  $2R$  is taken.

Figure 10 shows the evolution of the problem at a Reynolds number of 1250 for an initial separation between rings of  $1.0R$ . A new vortex ring is introduced every third sub-figure, starting with the first. As the solution progresses, the velocity fields of the vortices near the wall affect the velocities of the incoming rings and the distance between the rings changes. However, an initial height of  $2R$  ensures that the initial convection of the new vortex ring is unaffected by the previous vortices and their wall interactions. It is observed that the trajectories of the vortices right after injection are similar as the solution progresses, thus

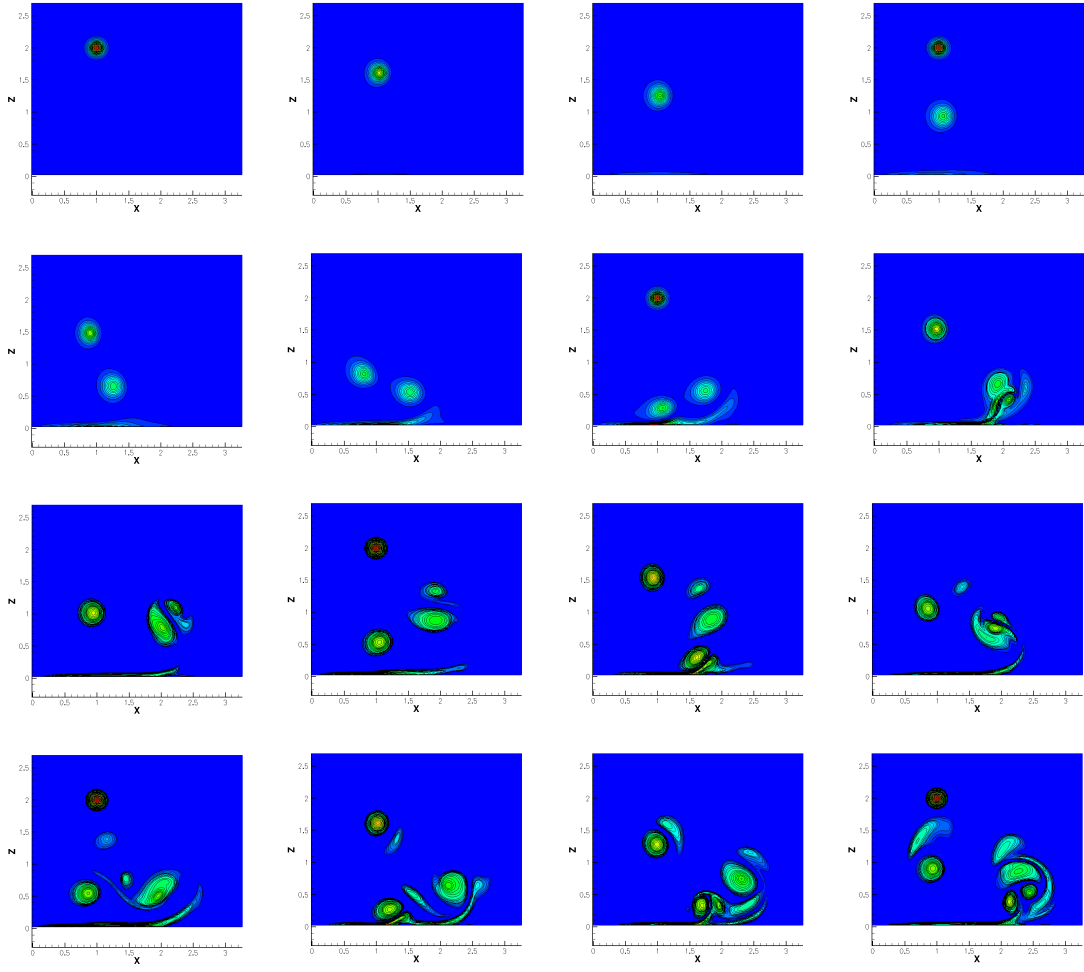


**Figure 10.** Multiple Ring Impingement at Reynolds number of 1250 and initial separation of  $1.0R$  (Time evolution is from left to right and top to bottom)

validating this assumption. The flow is solved on a  $300 \times 300 \times 200$  grid using the 5th order WENO scheme and 3rd order RK time stepping. Initially, the flow is similar to that of the impingement of two rings on a wall but it changes with the introduction of the third and subsequent rings. It is observed that whereas the earlier primary rings coalesce near the wall, the velocity field of the incoming rings force the coalesced structure away from the wall, thus reducing its influence on the boundary layer. The ejection of secondary vortices from the boundary layer is primarily caused by the incoming rings. The velocity field of the coalesced structure pushes the incoming rings towards the wall as was observed in the impingement of two rings. It is also observed that the trajectories of the secondary rings are not entirely determined by the primary ring that caused their ejection. The secondary vortex is expected to circle around the primary vortex due to the velocity field of the latter but an incoming vortex can cause it to break off from its previous trajectory and circle the incoming vortex. Near the wall, the flow is composed of several vortices interacting with each other. While diffusion causes the vortices to coalesce and form larger structures, the opposing velocity fields from nearby vortices can cause a distortion of the core for smaller vortices and eventual breaking apart to form two vortices. Figure 11 shows the flow for an initial separation between the rings of  $0.5R$  and it is observed that the above interactions are much more pronounced.

## VI. Conclusions

The impingement of multiple vortex rings on a solid wall is numerically studied in the present study. An incompressible flow solver based on the fractional step algorithm is used which solves the governing equations

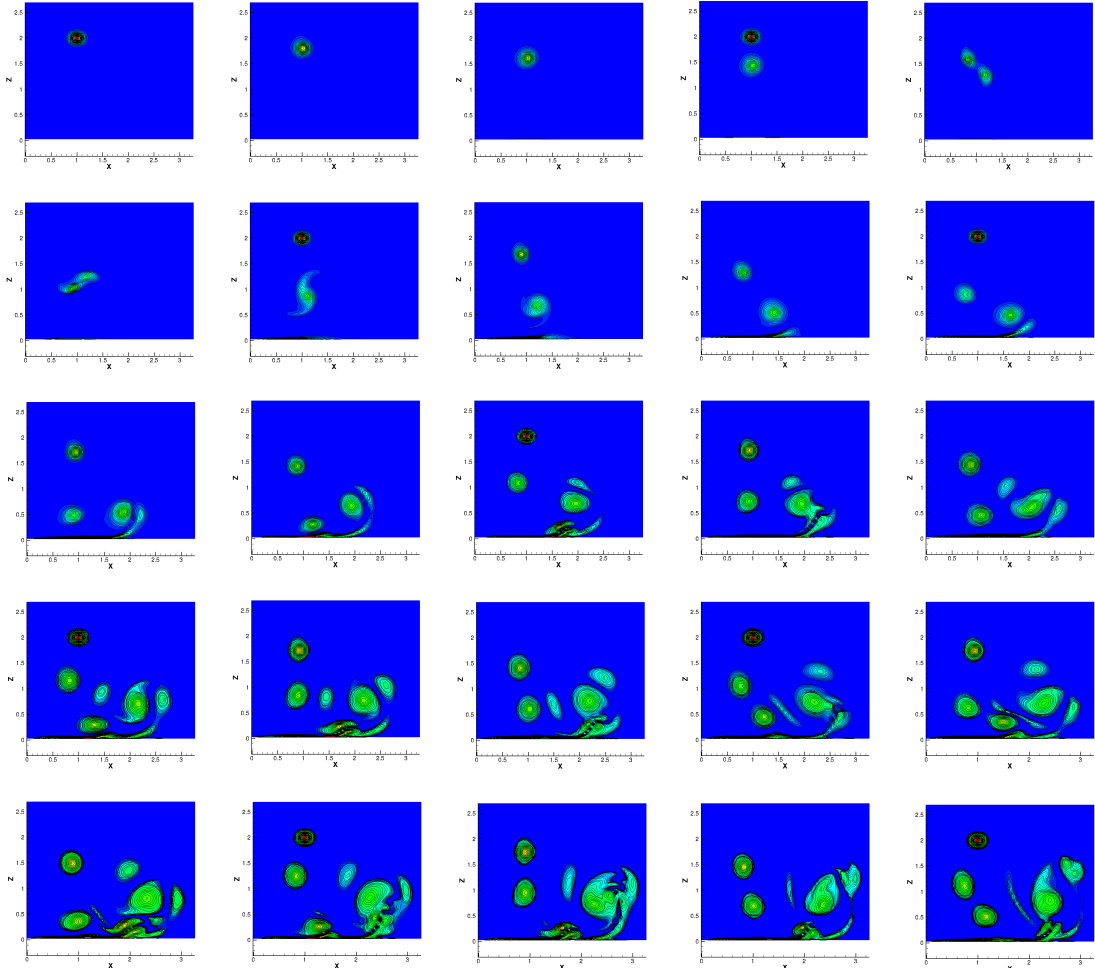


**Figure 11. Multiple Ring Impingement at Reynolds number of 1250 and initial separation of  $0.5R$  (Time evolution is from left to right and top to bottom)**

on a Cartesian staggered grid. An upwind flux reconstruction with high order WENO interpolation is used for the convective flux terms and central differencing is used for the viscous terms. The convective terms are evolved in time using the Runge-Kutta or the Adams-Bashforth schemes and the implicit trapezoidal scheme is used for the viscous terms to remove the time step restriction. The algorithm has been previously validated for benchmark incompressible flows. The algorithm is used to study vortex dominated flows for which previous results are available in literature. The focus is on flows with mutual interactions between vortex rings and their interactions with a solid wall since these are relevant to the present study. The inviscid leapfrogging of a pair of coaxial co-rotating vortex rings and the inviscid interaction of a vortex ring with a wall are simulated. The results are observed to be consistent with theoretical predictions. The viscous interactions of vortices with a wall is simulated and the results are compared with previous experimental/computational results. The two-dimensional case of a vortex dipole rebounding from a wall and the impingement of a three-dimensional vortex ring are studied and the results agree with those in literature.

Based on these results, the algorithm is used to simulate the impingement of two coaxial, co-rotating rings on a wall. The initial separation and the Reynolds number determine the behavior of the rings before their impingement. It is seen that for small separation and/or low Reynolds number, the rings coalesce to form a single ring before their impingement. In such a case, the behavior is qualitatively similar to that of an isolated ring but the interactions are stronger at the same Reynolds number. At higher Reynolds number and/or larger initial separation, the rings leapfrog while approaching the wall, which results in the initially leading ring pushing the initially trailing ring further into the boundary layer while getting pushed out itself.

The stronger collision of one of the primary vortices with the counter-rotating boundary layer vortex results in mutual weakening and the subsequent interactions between the primary vortices and the boundary layer are weaker. The viscous interaction of multiple rings is simulated for two different initial separations. In both these cases, it is observed that the incoming vortices push the primary vortices near the wall further out while they themselves are pushed closer to the boundary layer due to the preceding primary vortices. The incoming vortices are also observed to affect the trajectories of the secondary vortices whose motion is otherwise determined by the primary vortex that caused their ejection. It is also observed that while diffusion causes vortices to merge, opposing velocity fields from nearby vortices can cause core distortion and tearing of secondary vortices.

The flow simulated in the present study differs from the flow in a rotorcraft wake in two important respects. The vortices in the rotorcraft wake are helical filaments whereas the present study deals with axis-symmetric vortex rings. The wake of a rotorcraft has a strong downwash which dominate the convection of the vortices. In the present study, the convection of vortices are self-induced or due to mutual interactions. However, the results provide an insight in the interactions of vortices, especially near solid walls, which would be useful in understanding the wake flow for a rotorcraft operating in ground effect.

## References

- <sup>1</sup>Shariff, K., and Leonard, A., "Vortex Rings," *Annual Review of Fluid Mechanics*, Vol. 24, 1992, pp. 235-279
- <sup>2</sup>Cerra, A.W., and Smith C.R., "Experimental observations of vortex ring interaction with the fluid adjacent to a surface," Report FM-4, Department of Mechanical Engineering and Mechanics, Lehigh University, Bethlehem, PA
- <sup>3</sup>Verzicco R., and Orlandi P., "Wall/vortex-ring interactions," *Applied Mechanics Review*, Vol. 49, Issue 10, 1996, pp. 447-462
- <sup>4</sup>Sommerfield, A., *Mechanics of Deformable Bodies*, Lectures of Theoretical Physics Vol. II, Academic Press, New York, 1950
- <sup>5</sup>Riley, N., and Stevens, D.P., "A note on leapfrogging vortex rings," *Fluid Dynamics Research*, Vol. 11, 1993, pp. 235-244
- <sup>6</sup>Lim, T.T., "A note on the leapfrogging between two coaxial vortex rings at low Reynolds numbers," *Physics of Fluids*, Vol. 9, Issue 1, 1997, pp. 239-241
- <sup>7</sup>Walker, J.D.A., Smith C.R., Cerra A.W., and Doligalski T.L., "The impact of a vortex ring on a wall," *Journal of Fluid Mechanics*, Vol. 181, 1987, pp. 99-140
- <sup>8</sup>Magarvey, R.H., and MacLatchy, C.S., "The formation and structure of vortex rings," *Canadian Journal of Physics*, Vol. 42, 1964, pp. 678-689
- <sup>9</sup>Boldes U., and Ferreri J.C., "Behavior of vortex rings in the vicinity of a wall," *Physics of Fluids A*, Vol. 16, 1973, pp. 2005-2006
- <sup>10</sup>Yamada H., Hochizuki O., Yamabe H., and Matsui T., "Pressure variation on a flat induced by an approaching vortex ring," *Journal of the Physical Society of Japan*, Vol. 54, 1985, pp. 4151-4160
- <sup>11</sup>Liu, C.H., "Vortex simulation of unsteady shear flow induced by a vortex ring," *Computers & Fluids*, Vol. 31, 2002, pp. 183-207
- <sup>12</sup>Orlandi P., and Verzicco R., "Vortex impinging on walls: axissymmetric and three-dimensional simulations," *Journal of Fluid Mechanics*, Vol. 256, 1993, pp. 615-646
- <sup>13</sup>Ghosh, D., and Baeder, J.D., "A High Order Conservative Upwind Algorithm for the Incompressible Navier Stokes Equations," *40th AIAA Fluid Dynamics Conference and Exhibit*, AIAA-2010-5030, Chicago, IL, 2010
- <sup>14</sup>Temam, R., *Navier Stokes Equations*, North-Holland, Amsterdam, 1977
- <sup>15</sup>Ferziger, J.H., and Perric, M., *Computational Methods for Fluid Dynamics* (3<sup>rd</sup> Ed.), Springer, New York, 2002
- <sup>16</sup>Chung, T.J., *Computational Fluid Dynamics*, Cambridge University Press, Cambridge, 2002
- <sup>17</sup>Chorin, A.J., "A Numerical Method for Solving Incompressible Viscous Flow Problems," *Journal of Computational Physics*, Vol. 2, No. 1, 1967, pp. 12-26
- <sup>18</sup>Chorin, A.J., "Numerical Solution of the Navier Stokes Equations," *Mathematics of Computation*, Vol. 22, No. 104, 1968, pp. 745-762
- <sup>19</sup>Chorin, A.J., "On the Convergence of Discrete Approximation to the Navier-Stokes Equations," *Mathematics of Computation*, Vol. 23, No. 106, 1969, pp. 341-353
- <sup>20</sup>Kim, J., and Moin, P., "Application of a Fractional Step Method to Incompressible Navier-Stokes Equations," *Journal of Computational Physics*, Vol. 59, No. 2, 1985, pp. 308-323
- <sup>21</sup>Shu, C.W., and Osher S., "Essentially Non-Oscillatory and Weighted Essentially Non-Oscillatory Schemes for Hyperbolic Conservation Laws," ICASE 1997-65, 1995
- <sup>22</sup>Zedan, M., and Scheider G.E., "A Three-Dimensional Modified Strongly Implicit Procedure for Heat Conduction," *AIAA Journal*, Vol. 21, No. 2, 1983, pp. 295-303
- <sup>23</sup>Orlandi, P., "Vortex dipole rebound from a wall," *Physics of Fluids A*, Vol. 2, No. 8, 1990, pp. 1429-1436
- <sup>24</sup>Hahn S., and Iaccarino G., "Towards Adaptive Vorticity Confinement," *47th AIAA Aerospace Sciences Meeting*, AIAA-2009-1613, Orlando, FL, 2009